VSP

Advanced Composite Materials 18 (2009) 167–185

ADVANCED COMPOSITE MATERIALS
www.brill.nl/acm

Biodegradable Starch-Based Resin Reinforced with Continuous Mineral Fibres — Processing, Characterisation and Mechanical Properties

Thomas Wittek * **and Toshio Tanimoto**

Shonan Institute of Technology, Tsujido-Nishikaigan 1-1-25, Fujisawa, Kanagawa, 251-8511, Japan

Received 29 February 2008; accepted 11 June 2008

Abstract

Environmental problems caused by extensive use of polymeric materials arise mainly due to lack of landfill space and depletion of finite natural resources of fossil raw materials like petroleum or natural gas. The substitution of synthetic petroleum-based resins with natural biodegradable resins appears to be one appropriate measure to remedy the above-mentioned situation.

This study presents the development of a composite that uses environmentally degradable starch-based resin as matrix and natural mineral basalt fibres as reinforcement, and investigates the fibre's and the composite's mechanical properties. The tensile strength of single basalt fibres was verified by means of single fibre tensile tests and statistically investigated by means of a Weibull analysis. Prepreg sheets were manufactured by means of a modified doctor blade system and hot power press. The sheets were used to manufacture specimens with fibre volume contents ranging from 33% to 61%. Specimens were tested for tensile strength, flexural strength and interlaminar shear strength. Composites manufactured during this study exhibited tensile and flexural strength of up to 517 MPa and 157 MPa, respectively.

Keywords

'Green' composite, basalt fibres, biodegradable resin, processing, mechanical properties

1. Introduction

Many severe environmental issues arise due to extensive use of plastic. The most important positive characteristics of plastic, durability and light weight, change into severe drawbacks after disposal. If dumped into a landfill, plastic does not decompose and lose volume. As a result, the ground remains unstable and further use becomes difficult if not impossible. If plastic is burnt at a waste incineration plant, high energy consumption and the dispersal of harmful substances are only

* To whom correspondence should be addressed. E-mail: wittek@mate.shonan-it.ac.jp
Edited by JSCM

 DOI:10.1163/156855109X428808

two of the detrimental consequences. Additionally, the depletion of finite natural petrochemical resources, acceleration of the greenhouse effect, emission of toxic gases and damage to wildlife and marine species accompany the waste production process.

In an attempt to resolve these issues while creating an alternative for composites reinforced with synthetic fibres, research on 'green' composites has been conducted since at least the mid-1990s worldwide.

'Green' composites are defined as materials composed entirely, or in part, of constituents that are derived from renewable resources. This definition applies to both the reinforcement and matrix phases of the composites [1]. One crucial characteristic, which is common to most natural constituents used in 'green' composites, is biodegradability. Biodegradable composites are composed of biodegradable polymers and natural fibres in the majority of cases. Advantages of biodegradable composites include: biological degradation, reduction in the volume of garbage, compostability in the natural cycle, preservation of fossil-based raw materials, and protection of climate through reduction of carbon dioxide emission [2].

Natural fibres can be classified in several categories (Fig. 1). Most fibres that are currently used for manufacturing of 'green' composites are cellulose-based plant fibres. Although cellulose-based fibres possess several advantages, including low cost, low density, high specific properties and biodegradability, they exhibit some severe drawbacks. Some disadvantages of natural fibres are moisture absorption leading to fibre swelling, low thermal resistance, local or seasonal variations in quality, anisotropic fibre properties, and low compressive and transverse strength [3].

Taking these drawbacks into account and considering that it has been demonstrated that the greatest impact in environmental terms arises from the polymer matrix, which is usually derived from petrochemical resources, rather than from the reinforcement fibre [1], we have chosen to use environmentally degradable starch-

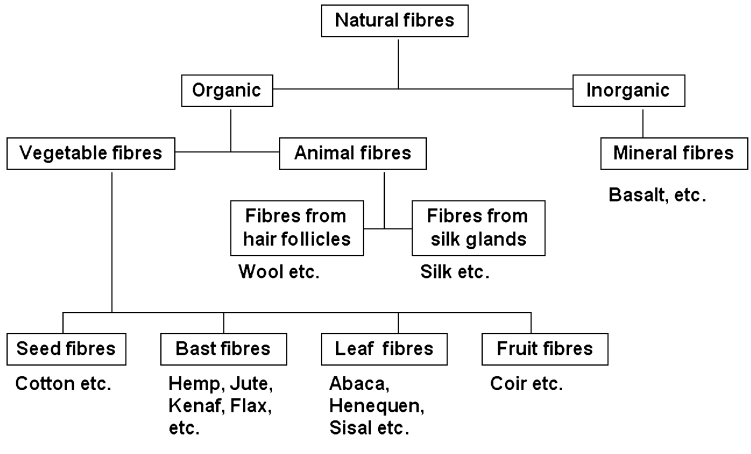

Figure 1. Classification of natural fibres (according to JIS L 0204-1: 1998).

based resin as matrix and natural mineral basalt fibres as reinforcement in this study. After verifying the single fibre tensile strength by means of single fibre tensile tests and Weibull analysis, we investigated the composites' basic mechanical properties in relation to modifications to the processing method and on variation of the fibre volume fraction.

2. Materials

2.1. Resin

Starch is an energy storage material occurring as granules in some plants and microorganisms. It is extracted from cereal seeds (maize, wheat, rice), tubers (potato) and roots (tapioca). The heating of starch granules with plasticiser in aqueous media results in gelatinisation caused by irreversible swelling of the granules. This leads to starch solubilisation as amylose leaches from the granules and amylopectin becomes fully hydrated. As starch products are moisture sensitive and brittle, it is necessary to modify starch or blend it with other materials in order to obtain commercially acceptable thermoplastic starch [4, 5].

In order to achieve high fibre content, we have chosen an emulsion type resin (Landy CP-300, Miyoshi Yushi Inc.) as matrix resin, in which fine resin particles of approximately 5 μm in diameter are dispersed in a water-based solution. CP-300 is based on starch and natural fatty acid ester. The starch is denaturised with fatty acid ester in order to achieve thermoplastic properties [6]. CP-300 has already been successfully applied with plant fibres such as abaca [7], curaua [8] and ramie [9]. The resin's properties are shown in Table 1.

2.2. Fibres

We have chosen basalt roving (BS-13-1200) with a filament diameter of 13 μm and linear weight of 1200 tex, and plain weave fabric (BT-8) produced by Sudaglass Fiber Technology Inc. (Russia) as reinforcement material during our research. The product properties of BT-8 are shown in Table 2.

The only ingredient used in the manufacture of basalt fibres is solidified volcanic lava, in which SiO_2 accounts for the main part, followed by Al_2O_3, then Fe_2O_3, FeO, CaO and MgO [12–14]. Basalt rocks are classified according to the SiO_2 content as alkaline (up to 42% SiO_2), mildly acidic (43% to 46% SiO_2) and acidic basalts (over 46% SiO_2). Only acidic type basalts satisfy the conditions for

Table 1.
Properties of starch resin CP-300 [10]

Density (g/cm^3)	1.17
Tensile strength (MPa)	8.3
Tensile elongation (%)	16.8
Elastic modulus (GPa)	0.3

Table 2.
Product properties of basalt plain weave fabric BT-8 [11]

Areal density (g/m^2)	Thickness (mm)	Warp density (yarns/cm)	Weft density (yarns/cm)
210	0.18	10	8

Table 3.
Comparison of mechanical properties of several synthetic and natural fibres

Material	Density (g/cm^3)	Tensile strength (MPa)	Elastic modulus (GPa)	Elongation at break (%)	Reference
Basalt	2.7	1430–3470	86–92	2.1–3.3	[12–16]
E-Glass	2.5	2000–3430	70–73	2.5–3.1	[18–20]
Flax	1.5	345–1100	28	2.7–3.2	[20]
Sisal	1.5	468–640	9.4–22	1.2–3.8	[20]

fibre preparation [15]. Basalt fibres are extruded from basalt rock through a melting process without application of any additives. The fibres are cost-effective and possess several excellent properties, such as outstanding sound and thermal insulation, non-flammability and good mechanical strength [12, 13, 16]. The mechanical properties of the basalt fibres are similar or superior compared to those of plant fibres and glass fibres (Table 3). Also, basalt fibre is environmentally and ecologically harmless, and free of carcinogens and other health hazards [17].

Although already known as an insulating material for almost 50 years, the possible applications of basalt fibres as a reinforcing material in polymer composites has only gained attention in recent years. Subramanian and Austin were the first to mention basalt fibres as a reinforcing agent for polymers in 1980 [21]. Since the mid 1990s, several reports have been published about basalt fibre-reinforced composites, but few have dealt with continuous fibres or fabrics as reinforcing agents. Ozawa *et al*. [22] investigated the tensile strength of cross-ply and unidirectional continuous basalt fibre reinforced phenolic and epoxy resin. Liu *et al*. [23, 24] investigated the mechanical properties and aging behaviour of basalt fibre composite for applications in transportation, where basalt twill weave reinforced epoxy and vinyl resin were the objects of the examination. Ye *et al*. [25] pioneered the combination of basalt fibres with biodegradable resin and reported the biodegradation behaviour of wheat gluten reinforced with unidirectional basalt yarn.

Burn-off tests indicated the basalt fibres were furnished with a proprietary sizing applied by the manufacturer. Although no information could be obtained about the nature of this sizing, initial test as described in this study were carried out with the fibre material in the state it was received.

3. Experimental

3.1. Processing

The manufacturing process combines the use of two kinds of processing equipment. Prepreg sheets are manufactured during the first processing stage. In order to manufacture these prepreg sheets, we have developed a production process using a doctor blade system (DP-150, Tsugawa Seiki Seisakusho Ltd.) in accordance with [26]. The sheets are subsequently subject to a thermo-mechanical moulding process, in which a hot power press (WF-37, Shinto Co.) comes into operation.

The doctor blade system consists of the doctor blade itself and a ground plate on which an electric propulsion device feeds a carrier film. The doctor blade consists of two blades, the primary and the secondary blades, which can be independently adjusted. Together with a diagonally attached slab, the primary blade forms a reservoir for the resin (Fig. 2).

Fibres, attached to a carrier film, are fed on the ground plate at a carrier speed of 30 cm/min. They pass beneath the two blades, while resin-emulsion is poured into the reservoir. After drying overnight and being cut to size, the preliminary sheets were subjected to an initial pressure and heat application process (prepreg moulding), turning them into prepreg sheets (Fig. 3). Afterwards, several layers of prepreg sheets were stacked and subjected again to a pressure and heat application process (sample moulding) using a hot power press. Spacers were used during sample moulding to achieve a predefined sample thickness. The manufacturing process is shown in Fig. 4.

The specifications and parameters for the moulding procedure were decided upon after extensive literature review of the existing moulding methods for similar resin systems [7, 8, 27–29]. The initial processing scheme was identical for both moulding processes. After putting the sheets onto the lower plunger of the hot press, the heating device was engaged and the sheets heated until they reached a processing temperature of 150°C. Marginal pressure was then applied for 30 minutes to enable

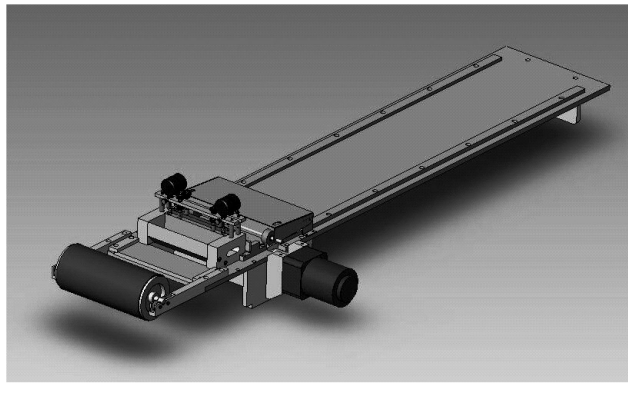

Figure 2. Doctor blade system.

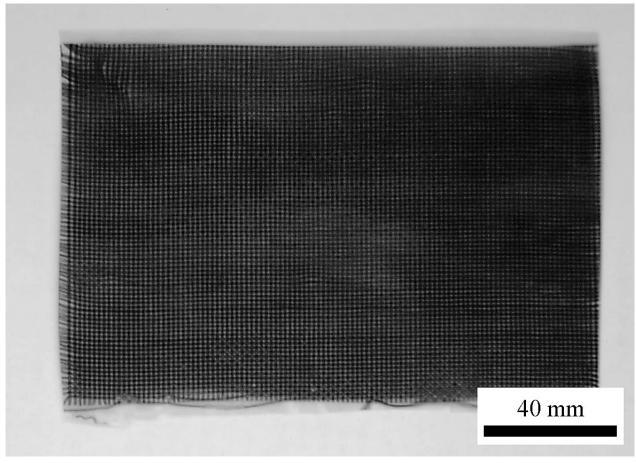

Figure 3. Basalt fabric reinforced prepreg sheet sample.

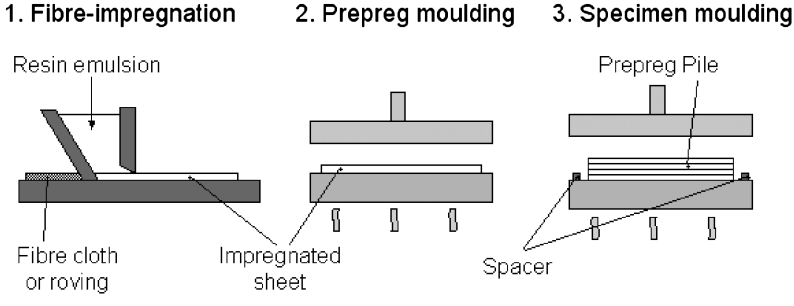

Figure 4. Composite manufacturing process.

the trapped air to escape and to facilitate the impregnation of the matrix among the fibres. The pressure was subsequently increased to 4.9 MPa, while the heating device was switched off, allowing the sample to cool to room temperature, at a rate of approximately 0.5°C/min.

Unidirectional samples were manufactured using basalt roving, and bidirectional samples were manufactured using basalt plain weave fabric. After producing unidirectional tensile and flexural samples with the initial processing parameters, the temperature and pressure for the prepreg moulding process were changed for tensile test sample production to 130°C and 170°C, and to 9.8 MPa, respectively, in order to determine the influence of the prepreg moulding processing parameters on the properties of the final specimens. All unidirectional tensile test samples were manufactured with 4 layers of prepreg sheets; flexural test samples were manufactured with 8 layers.

In order to determine the influence of the volume fibre fraction on the mechanical properties, textile composite samples were produced with varying numbers of prepreg sheets. The number of prepreg sheet layers used to manufacture tensile test

Table 4.
Processing parameters for tensile test specimen production

Fibre type	Basalt roving (BS-13-1200)				Basalt fabric (BT-8)			
Prepreg moulding temperature (°C)	130	150	170	150	150			
Prepreg moulding pressure (MPa)	4.9	4.9	4.9	9.8	4.9			
Sample moulding temperature (°C)	150				150			
Sample moulding pressure (MPa)	4.9				4.9			
Number of prepreg sheet layers (1)	4				4	5	6	7

Table 5.
Processing parameters for flexural test specimen production

Fibre type	Basalt roving (BS-13-1200)	Basalt fabric (BT-8)				
Prepreg moulding temperature (°C)	150	150				
Prepreg moulding pressure (MPa)	4.9	4.9				
Sample moulding temperature (°C)	150	150				
Sample moulding pressure (MPa)	4.9	4.9				
Number of prepreg sheet layers [1]	8	6	8	9	10	12

specimens ranged from 4 to 7, while the 6 to 12 layers of prepreg sheets were used to manufacture flexural test specimens. All bidirectional samples were manufactured with a temperature of 150°C and a pressure of 4.9 MPa in both processing stages. Processing parameters are summarised in Tables 4 and 5.

3.2. Determination of Tensile Properties

An Instron universal material-testing machine, model 4200, was used for the tension tests. The tests were carried out according to JIS K 7113 with a displacement rate of 1.0 mm/min. All samples had a length of 200 mm, a width of 10 mm and a thickness of 1 mm. End tabs with chamfered edges and manufactured of cross-plied glass fibre reinforced epoxy resin were attached to the specimens using an appropriate adhesive to avoid untimely rupture at the load transmission points. The tensile strength σ_M and elastic modulus E_M were calculated from (1) and (2), where A is the specimens' cross-sectional area, F_M the maximum tensile load, ε_1 and ε_2 tensile strain values of 0.0005 and 0.0025, and σ_1 and σ_2 tensile stress values measured at ε_1 and ε_2.

$$\sigma_M = \frac{F_M}{A}, \tag{1}$$

$$E_M = \frac{\sigma_2 - \sigma_1}{\varepsilon_2 - \varepsilon_1}. \tag{2}$$

During the tests the initiated load was recorded by the attached computer system, while the tensile strain was quantified by means of strain gauges.

3.3. Determination of Flexural Properties

A Shimadzu AGS-1000B universal material-testing machine was used for the flexural tests. The tests were carried out according to JIS K 7017 as 3-point-bending tests, with a displacement rate of 1.0 mm/min. Samples had a length of 60 mm, a width of 15 mm and a thickness of 2 mm. The flexural strength σ_{fm} and flexural modulus E_{f} were calculated according to (3) and (4), where b and h are the specimens' width and thickness, L is the span length, S is deflection and F_{m} is load. ΔS and ΔF were calculated from (5) and (6), where F' and F'' are the loads corresponding to the deflections S' and S''.

$$\sigma_{\mathrm{fm}} = \frac{3F_{\mathrm{m}}L}{2bh^2}, \tag{3}$$

$$E_{\mathrm{f}} = \frac{L^3}{4bh^3}\left(\frac{\Delta F}{\Delta S}\right), \tag{4}$$

$$\Delta S = S'' - S' = \frac{\varepsilon''_{\mathrm{f}}L^2}{6h} - \frac{\varepsilon'_{\mathrm{f}}L^2}{6h} = \frac{0.0025L^2}{6h} - \frac{0.0005L^2}{6h}, \tag{5}$$

$$\Delta F = F'' - F'. \tag{6}$$

During the tests the initiated load was recorded by an attached computer system; the flexural strain was quantified by means of strain gauges.

3.4. Determination of Interlaminar Shear Strength

Apparent interlaminar shear strength was determined according to the JIS K 7057 standard using the short beam method with a Shimadzu AGS-1000B universal material-testing machine. Samples had a length of 20 mm, a width of 10 mm and a thickness of 2 mm. The displacement rate was set at 1 mm/min. The interlaminar shear strength τ_{M} was calculated from (6), where b and h are the specimens' width and thickness, and F_{M} is the maximum load.

$$\tau_{\mathrm{M}} = \frac{3}{4}\left(\frac{F_{\mathrm{M}}}{bh}\right). \tag{7}$$

3.5. Determination of Geometrical and Tensile Properties of Single-Filament Specimens

In order to confirm the fibres tensile properties, single fibres were extracted from fibre bundles to carry out tensile tests according to JIS R 7607. Twenty samples were produced by fixing single fibres with a length of at least 45 mm to paper holders with slots of 25 mm length, which is correspondent to the gauge length, as seen in Fig. 5. Each sample was attached to a Shimadzu AGS-1000B universal material-testing machine, equipped with a 50 N load cell. After cutting the paper holder, specimens were subjected to the tensile test with a displacement rate of 0.5 mm/min.

The filament diameter and the cross-sectional area were determined based on scanning electron microscope surveys of fibre fragments recovered after the tensile

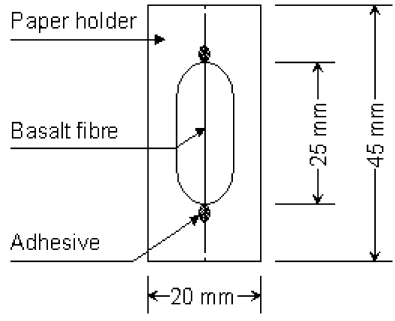

Figure 5. Single-filament tensile test specimen.

tests. Tensile strength σ_f was calculated from (8), where F_f is the maximum tensile load and A_f the filament cross-sectional area.

$$\sigma_f = \frac{F_f}{A_f}. \tag{8}$$

3.6. Examination of Microstructural Characteristics

The fractured surfaces of the specimen were examined using a scanning electron microscope (SEM, Hitachi S-2100 A). Specimens were gold coated prior to the examination, using a Hitachi E101 ion sputter, to achieve sufficient electrical conductivity.

4. Test Results

4.1. Properties of Single Basalt Fibres

Table 6 shows the mean results for tensile strength, elongation at break and fibre diameter of basalt fibres. In order to characterise the fibre properties more accurately, the tensile strength values were subjected to a Weibull analysis [30]. The Weibull distribution, which is usually used to describe the distribution of the fibre strength, is based on the weakest link theory in which failure of the most serious flaw leads to the catastrophic fracture of the entire material.

In order to evaluate the dependence of fibre diameter on tensile strength the strength was plotted as a function of the diameter (Fig. 6). Looking at Fig. 6, it is reasonable to assume that no relationship exists between fibre diameter and fibre strength. A linear correlation analysis using Equation (9) was conducted, where r is the correlation coefficient, d_i and σ_{fi} are the individual values, and $\overline{d}$ and $\overline{\sigma}_f$ the mean values of fibre diameter and strength, respectively.

$$r = \frac{\Sigma(d_i - \overline{d})(\sigma_{fi} - \overline{\sigma}_f)}{\sqrt{\Sigma(d_i - \overline{d})^2}\sqrt{\Sigma(\sigma_{fi} - \overline{\sigma}_f)^2}}. \tag{9}$$

The analysis yielded a coefficient value of $r = -0.0841$, proving a weak linear relationship between diameter and strength. As a result, it was decided not to

Table 6.
Mean results of the single basalt fibre tensile tests

Fibre diameter (μm)	13.1
Tensile strength (MPa)	1540
Elongation at break (%)	2.6

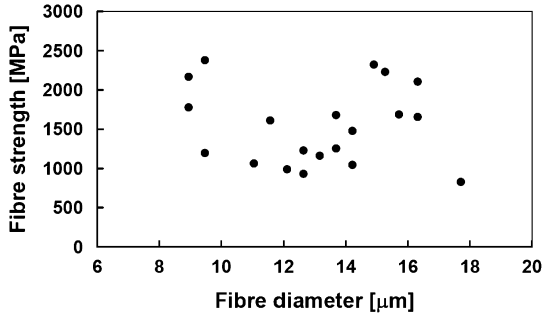

Figure 6. Scatter plot of fibre strength *versus* fibre diameter.

take the fibre diameter variation into account for the Weibull analysis of the fibre strength.

Assuming further the location parameter to be zero, a two-parameter Weibull distribution was chosen for this analysis, with the cumulative density function set as follows

$$P(\sigma_f) = 1 - \exp\left(-\left(\frac{\sigma_f}{\sigma_0}\right)^m\right), \tag{10}$$

where P is the failure probability of the fibre, σ_f is the measured tensile strength, m is the shape parameter and σ_0 the scale parameter of the distribution.

Equation (10) was modified to the following form for the Weibull plot (Fig. 7).

$$\ln\ln\left(\frac{1}{1 - P(\sigma_f)}\right) = m\ln\sigma_f - m\ln\sigma_0. \tag{11}$$

The mean fibre strength $\mu(\sigma_f)$ was obtained from (12), while the standard deviation $\sigma(\sigma_f)$ was calculated from (13):

$$\mu(\sigma_f) = \sigma_0\Gamma\left(1 + \frac{1}{m}\right), \tag{12}$$

$$\sigma(\sigma_f) = \sigma_0\left(\Gamma\left(1 + \frac{2}{m}\right) - \Gamma^2\left(1 + \frac{1}{m}\right)\right)^{1/2}, \tag{13}$$

where Γ is the Gamma Function. The Weibull parameters are shown in Table 7.

The line of the Weibull plot fits the experimental data fairly well, and the applied Weibull distribution shows a rather small dispersion and is close to the normal distribution, as indicated by the value of the shape parameter m.

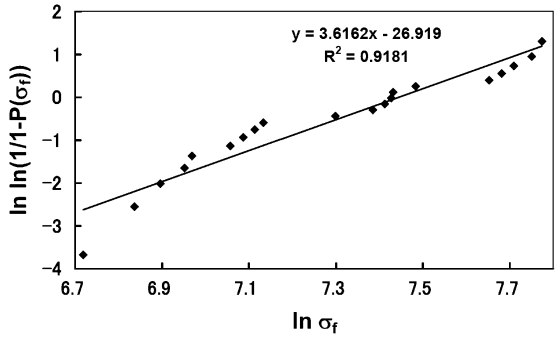

Figure 7. Weibull plot (double natural logarithm of failure probability *versus* logarithmic fibre strength).

Table 7.
Weibull parameters for the single basalt fibre tensile strength

m	σ_0 (MPa)	Mean strength (MPa)	Standard deviation (MPa)
3.62	1709	1544	427

4.2. Mechanical Properties of Unidirectional Reinforced 'Green' Composite

Samples manufactured with the initial prepreg moulding parameters of 150°C and 4.9 MPa were tested for tensile strength, flexural strength and interlaminar shear strength. The results are summarised in Table 8, while typical tensile and flexural stress–strain diagrams are shown in Fig. 8.

A variety of analytical models is available in the literature to evaluate the tensile strength of continuously reinforced composite materials. The most popular approaches are the rule of mixture model [31] and statistical models, such as the bundle strength theory [32]. In statistical models, the composite failure is treated based on the statistical distribution of flaws or imperfections in the fibres. For the estimation of tensile strength of UD laminates, the rule of mixture model is simple and reasonably accurate. The tensile strength σ_{1c} can be predicted using the following equation

$$\sigma_{1c} = (1 - V_f)\sigma_{1m} + V_f\sigma_{1f}, \tag{14}$$

while the elastic modulus can be displayed using the following equation

$$E_{1c} = E_f\left(\frac{(1 - V_f)\sigma_{1m}}{\sigma_{1f}} + V_f\right), \tag{15}$$

where σ and E indicate stress and elastic modulus, respectively. V_f is the fibre volume fraction and indices c, m and f refer to composite, matrix and fibre, respectively.

Table 8.
Mechanical properties of unidirectional reinforced composite

Prepreg moulding pressure (MPa)	4.9
Prepreg moulding temperature (°C)	150
Sample moulding pressure (MPa)	4.9
Sample moulding temperature (°C)	150
Fibre volume fraction (%)	40
Tensile strength (MPa)	517
Elongation at break (%)	2.0
Elastic modulus (GPa)	31.8
Flexural strength (MPa)	157
Flexural modulus (GPa)	16.9
Interlaminar shear strength (MPa)	7.9

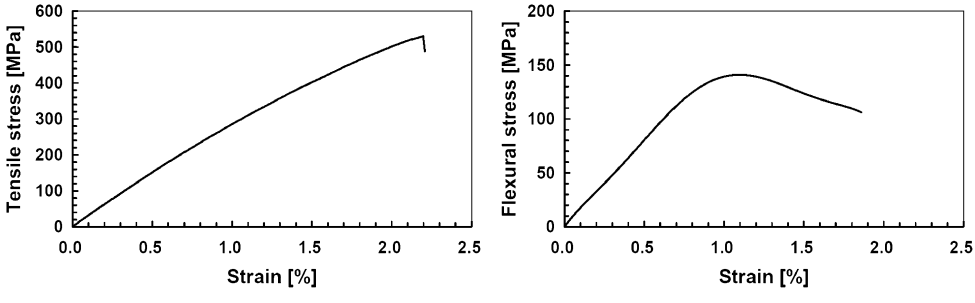

Figure 8. Typical tensile (left) and flexural (right) stress–strain diagrams of unidirectional reinforced composites with 40% volume fibre fraction.

The predicted tensile strength and the elastic modulus for the unidirectional composite laminae were 621.0 MPa and 34.7 GPa, respectively. While the actual value of the elastic modulus was within 92% to the predicted value, the actual tensile strength was only 83% of the predicted value.

Although fibres can be oriented parallel to external tensile loads, it is almost impossible to avoid transverse stresses, which present a major problem in unidirectional laminae. Due to relatively small matrix-dependent transversal strength and stiffness, transverse stresses in unidirectional laminates may lead to premature failure.

All unidirectional composite samples in this study were produced by aligning basalt roving by hand. As the fibre orientation is not completely parallel, the possibility of premature failure increased. As a result, the unidirectional composite specimens were fractured by premature matrix failure as can be seen in Fig. 9.

An important attribute of the rule of mixtures is the assumption of a strong fibre–matrix bond. As is apparent by the low value of the interlaminar shear strength of only 7.9 MPa, the adhesion between the laminae and between fibres and matrix in the interlaminar area is not really sufficient. This low value further promotes a

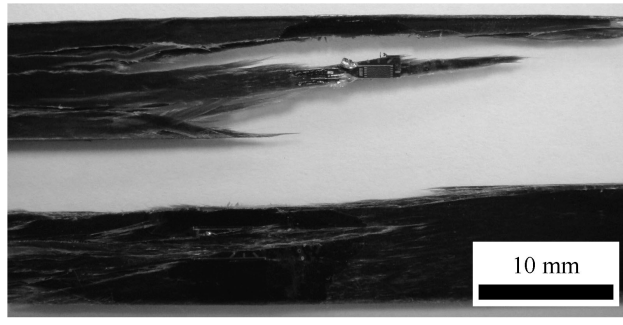

Figure 9. Fractural behaviour of unidirectional composite.

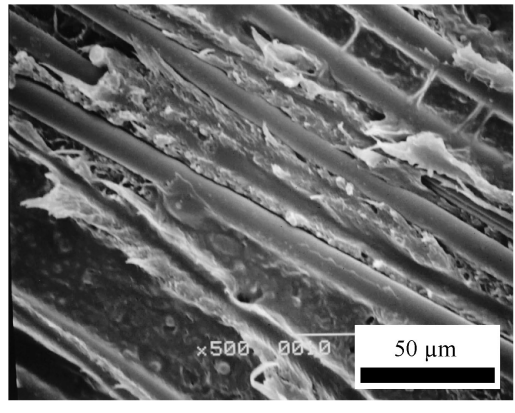

Figure 10. SEM-micrograph of the interlaminar fracture surface.

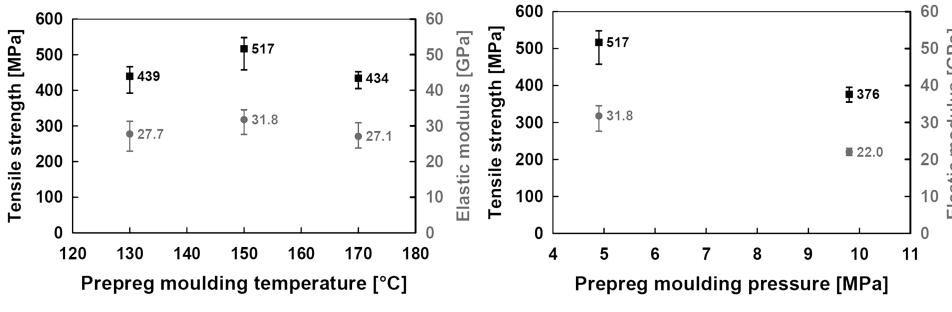

Figure 11. Effect of processing temperature (left) and pressure (right) on the tensile properties.

premature matrix failure. Fibre debonding in the interlaminar area is visible in the SEM micrograph of the interlaminar fracture surface (Fig. 10).

The effect of the processing temperature on the mechanical properties of the unidirectional composite is shown in the left side of Fig. 11. The tensile strength and the elastic modulus were increased by means of a processing temperature increase from 130°C to 150°C. This may be attributed to better fibre wetting and more thor-

ough fibre impregnation through lower resin viscosity. A further increase of the processing temperature to 170°C led to a decrease in the tensile strength. This behaviour is suggests possible damage to the resin matrix due to high temperature. Another feasible explanation for the decrease in tensile strength is based on thermal residual stresses, which arise due to the mismatch in coefficients in thermal expansion between the basalt fibres and the thermoplastic matrix. The effect of the processing pressure on the mechanical properties of the unidirectional composite is shown in the right side of Fig. 11. An increase in processing pressure from 4.9 MPa to 9.8 MPa led to a decrease in tensile strength, which may have been caused by increased misalignment of the fibres in the loading direction. On the basis of the above-mentioned results, 150°C and 4.9 MPa were selected as processing parameters at both moulding stages for the manufacturing of subsequent specimens.

4.3. Mechanical Properties of Bidirectional Reinforced 'Green' Composite

Typical tensile and flexural stress strain diagrams of plain-weave composite are shown in Fig. 12. Basalt fibre plain-weave reinforced 'green' composites with up to 60% fibre volume fraction and with a tensile strength of more than 370 MPa and a flexural strength of about 120 MPa have been manufactured successfully.

Figure 13 presents the tensile strength and the elastic modulus of the plain weave reinforced composite against the fibre volume content. The tensile strength of the composite already achieves a value of 281 MPa with a volume fibre content of 32%. An increase in the fibre volume fraction up to 50% leads to an increase in tensile strength to 366 MPa, but once the fibre volume content exceeds 50% and reaches up to 61%, the tensile strength value remains almost constant at 373 MPa.

These tensile strength properties can be explained by non-sufficient fibre wetting, which increases at higher volume fractions. Comparing the fracture behaviour of a 33% sample and a 50% sample, it is evident that the former shows an almost linear fracture surface, while the later exhibits a rather brush-like appearance, which suggests an increased fibre pull-out (Fig. 14). A further indicator for decreased fibre wetting and a decreased fibre-resin-bond is the SEM micrograph (Fig. 15) of the fracture surface of the 50% sample. The resin did not penetrate the fibre bundles sufficiently. A sufficient fibre–matrix-bond only took place partially on the outer fibres of the bundles; however with the fibres inside the bundles touching each other, an increase in fibre pull-out resulted. Also evident from the SEM micrograph is the relatively high void content. The presence of voids in the composite is a further factor that accounts for debonding and premature failure of composites.

The behaviour of the elastic modulus in tension against the change of the fibre volume content is similar to the behaviour of the tensile strength. The elastic modulus value of 11.8 GPa, which was achieved with a fibre volume fraction of 32%, initially went up as expected with the increase in the fibre volume fraction to 17.3 GPa at 50%. The modulus value, however, dropped to 15.8 GPa, notwithstanding an increase of the fibre volume fraction to 61%. The slightly increasing, and subsequently even decreasing values of the elastic modulus may be assigned

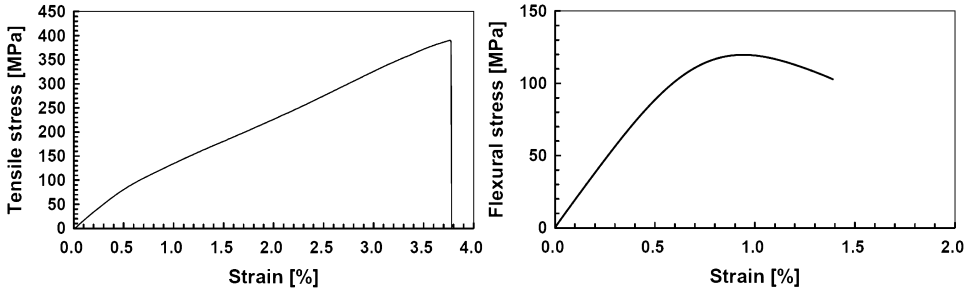

Figure 12. Typical tensile (left, $V_f = 61\%$) and flexural (right, $V_f = 42\%$) stress–strain diagrams of plain weave reinforced composites.

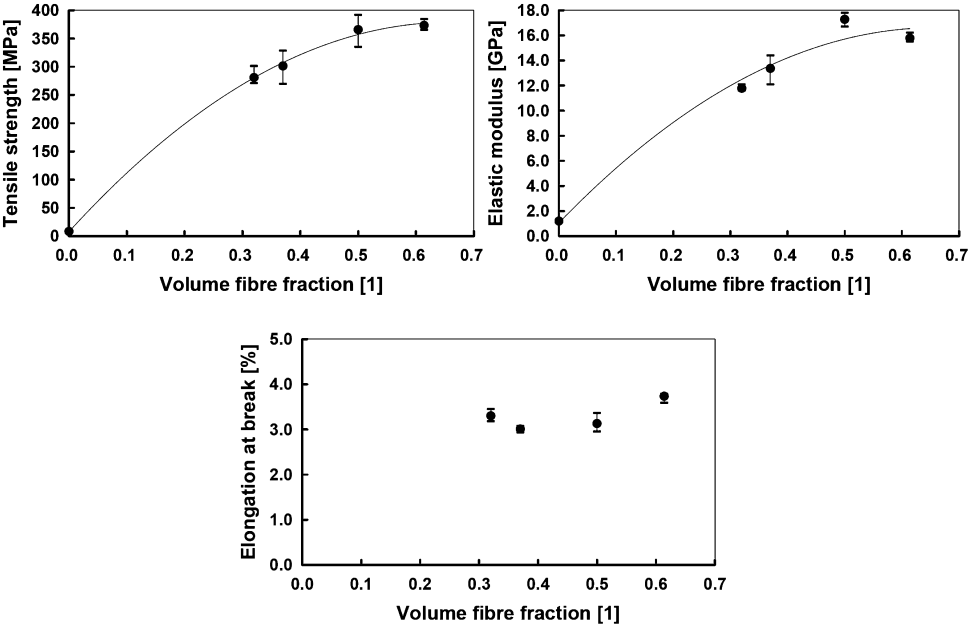

Figure 13. Tensile properties *versus* fibre volume content.

to the higher void content and low interfacial shear strength, which resulted in less efficiency of load transfer with the increase of fibre content.

Figure 13 also presents the fracture strains of the composites as a function of the fibre volume content, where we can see that strain values are independent of the fibre content. The maximum value of 3.74% at a volume fibre content of 61% is slightly higher than the maximum fracture strength values reported for single basalt fibres. Such behaviour demonstrates that the fibres are the main load-bearing component, and points out that an improvement of the fibre–matrix bonding properties is necessary in order to achieve higher fracture strain values at higher fibre volume contents, and consequently an overall improvement of the tensile properties.

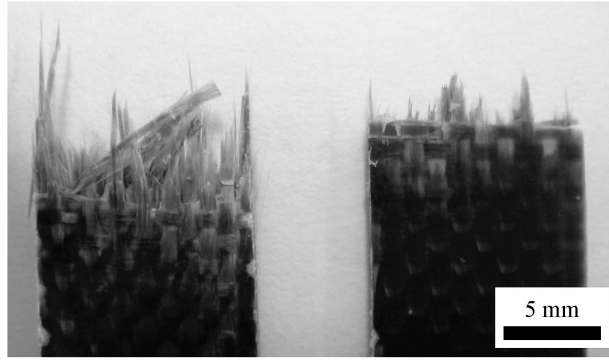

Figure 14. Fracture behaviour of woven cloth composite specimens; left: $V_f = 50\%$, right: $V_f = 32\%$.

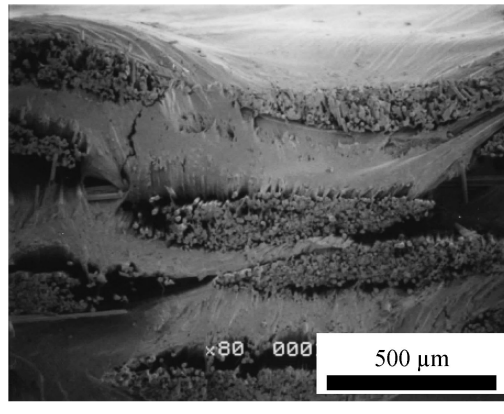

Figure 15. SEM micrograph of the fracture surface of a woven cloth composite with $V_f = 50\%$.

Figure 16 shows the flexural strength, flexural modulus and flexural strain at yield against the fibre volume fraction. The flexural strength and the flexural modulus show a steady linear rise with the increase in fibre content. The flexural strength rises from 73 MPa at $V_f = 24\%$ to 122 MPa at $V_f = 51\%$, and the flexural modulus increases within the same range of fibre content from 9.7 GPa to 19.7 GPa. Furthermore, with the increase of the fibre content we are able observe an increase in the flexural stiffness, indicated by a tendency of slightly decreasing flexural strain values, ranging between 1.35% and 1.03%.

During the three point-bending test, the lower layers are under tension and the upper layers are subject to compression. As shown in Fig. 17, all flexural samples exhibited compressive fracture caused by fibre buckling failure. Buckling of fibres is mainly restricted by the surrounding matrix and, therefore, dependent on resin properties and the quality of fibre–matrix bond. As debonded fibres buckle more readily then well-bonded fibres, it is obvious that improvement of the interfacial bonding strength will lead to an improvement of the flexural properties.

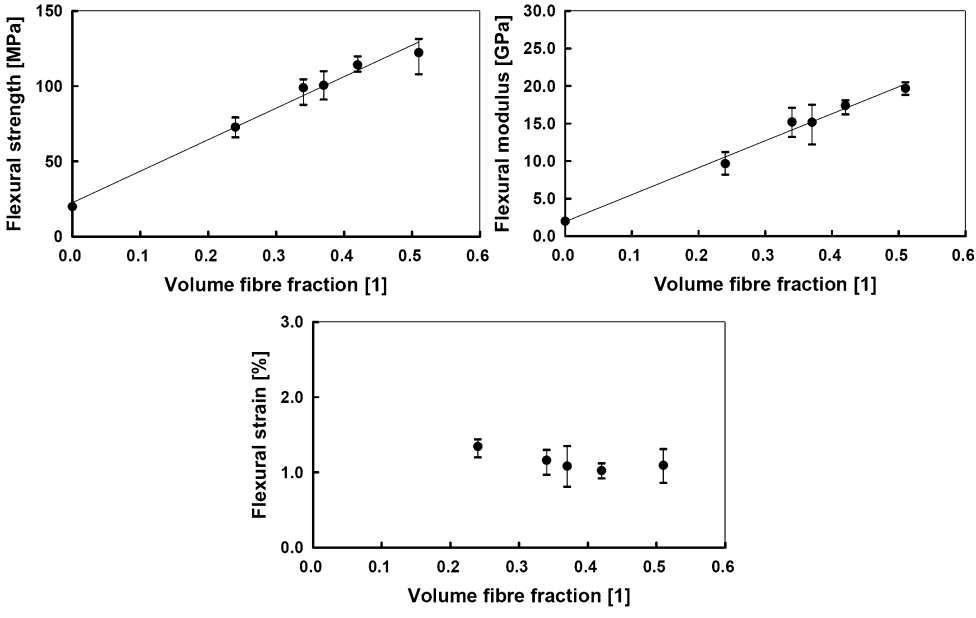

Figure 16. Flexural properties *versus* fibre volume content.

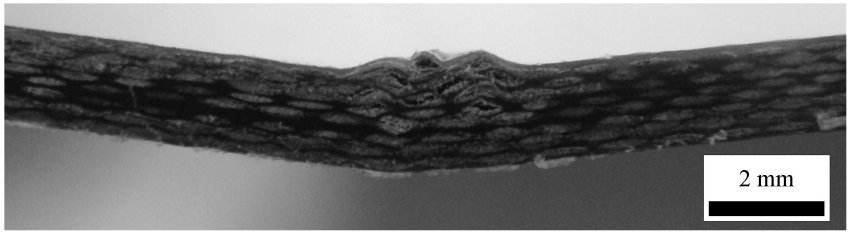

Figure 17. Flexural failure mode of basalt weave-reinforced specimen.

5. Conclusions and Considerations

(1) By use of basalt roving and woven basalt cloth with starch resin, high strength, unidirectional 'green' composites and high strength, two-ply 'green' composites have been successfully manufactured through the utilisation of hot press machinery and a doctor blade system.

(2) Through application of the doctor blade system, the fabrication process was successfully automated to a high degree.

(3) Through the analysis of the mechanical properties in relation to the volume fibre content, we have verified that tensile and flexural strength, as well as the according moduli, can be enhanced by increasing fibre content. The enhancement of the properties is, however, not as continuous as desired, while the strain behaviour is largely independent of the fibre content. This behaviour indicates that the fibres are the predominant load-bearing component, especially at higher fi-

bre fractions, and that the fibre–matrix bond still leaves room for improvement. A further sign of suboptimal fibre–matrix bond is the dominance of compressive fracture at the flexural tests. A relatively high void content was identified as a further factor. The actual characteristics of the composites offer, therefore, the opportunity to improve interfacial bonding strength and other properties even further by the use of chemical treatments.

Due to their favourable mechanical properties and limited impact on the environment, mineral basalt fibres are a promising alternative as reinforcing agents in 'green' composites. Although further steps should be taken to improve the composite properties, basalt fibre reinforced biodegradable 'green' composites already show above-average mechanical properties. As one measure to enhance interfacial bonding strength and fibre wettability, the use of surface treatment is being investigated and results will be reported in the future. Further improvement of the manufacturing process, as well as an analysis of the recyclability of the reinforcement phase, will be the focus of future research in order to broaden the applicability of basalt fibres as reinforcement in environmentally friendly composites.

Acknowledgement

The authors gratefully acknowledge financial support by the Itoyama International Foundation and the Rotary Yoneyama Memorial Foundation.

References

1. M. Hughes, in: *Green Composites: Polymer Composites and the Environment*, C. Baille (Ed.), pp. 233–251. Woodhead Publishing, Cambridge (2004).
2. M. Sain and S. Panthapulakkal, in: *Green Composites: Polymer Composites and the Environment*, C. Baille (Ed.), pp. 181–205. Woodhead Publishing, Cambridge (2004).
3. A. Stamboulis, C. Baille and T. Peijs, Effects of environmental conditions on mechanical and physical properties of flax fibers, *Composites: Part A* **32**, 1105–1115 (2001).
4. D. Plackett, in: *Green Composites: Polymer Composites and the Environment*, C. Baille (Ed.), pp. 123–153. Woodhead Publishing, Cambridge (2004).
5. B. S. Chiou, G. M. Glenn, S. H. Imam, M. K. Inglesby, D. H. Wood and W. J. Orts, in: *Natural Fibers, Biopolymers and Biocomposites*, A. K. Mohanty, M. Misra and L. T. Drzal (Eds), pp. 639–670. Taylor & Francis, Boca Raton, FL (2005).
6. H. Tanaka, Denpun emarujon randi, *Engineering Materials* **51**, 58–62 (2003) (in Japanese).
7. S. Ochi, H. Takagi and H. Tanaka, Development of High-Strength Cross-Ply "Green" Composites, *Zairyo* **52**, 857–862 (2003) (in Japanese).
8. A. Gomes, K. Goda and J. Ohgi, Effects of alkali treatment to reinforcement on tensile properties of curaua fiber green composites, *JSME International Journal, Series A* **47**, 541–546 (2004).
9. T. Uno, N. Suizu, K. Goda and J. Ohgi, Tensile and impact properties of mercerized ramie fiber green composite, in: *Proc. 4th Intern. Workshop on Green Composites (IWGC-4)*, Tokyo, Japan, pp. 147–149 (2006).
10. T. Wittek and T. Tanimoto, Comparison of tensile properties of starch resin reinforced with natural and synthetic fibres, in: *Proc. 4th Int. Workshop on Green Composites (IWGC-4)*, Tokyo, Japan, pp. 112–115 (2006).

11. Available at www.sudaglass.com
12. D. Z. Dzhigiris, M. F. Makhova, V. D. Gorobinskaya and L. N. Bombyr, Continuous basalt fiber, *Glass and Ceramics* **40**, 467–470 (1983).
13. N. N. Morozov, V. S. Bakunov, E. N. Morozov, L. G. Aslanova, P. A. Granovskii, V. V. Prokshin and A. A. Zemlyanitsyn, Materials based on basalts from the European North of Russia, *Glass and Ceramics* **58**, 100–104 (2001).
14. M. A. Sokolinskaya, L. K. Zabava, T. M. Tsybulya and A. A. Medvedev, Strength properties of basalt fibers, *Glass and Ceramics* **48**, 435–437 (1991).
15. J. Militky and V. Kovacic, Ultimate mechanical properties of basalt filaments, *Textile Research Journal* **66**, 225–229 (1996).
16. V. V. Gur'ev, E. I. Neproshin and G. E. Mostovoi, The effect of basalt fiber production technology on mechanical properties of fiber, *Glass and Ceramics* **58**, 62–65 (2001).
17. F. M. Kogan and O. V. Nikitina, Solubility of chrysotile asbestos and basalt fibers in relation to their fibrogenic and carcinogenic action, *Environmental Health Perspectives* **102** Supplement 5, 205–206 (1994).
18. F. L. Matthews and R. D. Rawlings, *Composite Materials: Engineering and Science.* Chapman and Hall, London (1994).
19. N. Nanjyo, FRP kosei sozai nyumon dai 2 sho: Garasu seni, *Journal of the Japan Society for Composite Materials* **33**, 141–149 (2007) (in Japanese).
20. A. K. Mohanty, M. Misra and G. Hinrichsen, Biofibres, biodegradable polymers and biocomposites: an overview, *Macromolecular Materials and Engineering* **276/277**, 1–24 (2000).
21. R. V. Subramanian and H. F. Austin, Silane coupling agents in basalt-reinforced polyester composites, *Int. J. Adhesion and Adhesives* **1**, 50–54 (1980).
22. Y. Ozawa, T. Kikuchi and M. Isohata, Mechanical behavior of basalt fiber reinforced polymer composites in temperature conditions, in: *Proc. 3rd Intern. Workshop on Green Composites (IWGC-3)*, Kyoto, Japan, pp. 124–127 (2005).
23. Q. Liu, M. T. Shaw, R. S. Parnas and A. M. McDonell, Investigation of basalt fiber composite mechanical properties for applications in transportation, *Polym. Compos.* **27**, 41–48 (2006).
24. Q. Liu, M. T. Shaw, R. S. Parnas and A. M. McDonell, Investigation of basalt fiber composite aging behavior for applications in transportation, *Polymer Composites* **27**, 475–483 (2006).
25. P. Ye, L. Reitz, C. Horan and R. Parnas, Manufacture and biodegradation of wheat gluten/basalt composite material, *J. Polymers and the Environment* **14**, 1–7 (2006).
26. T. Tanimoto, Continous-fibre CMC fabrication by using pre-impregnated sheets, *Composites: Part A* **30**, 583–586 (1989).
27. M. Dauda and M. Yoshiba, Processing and mechanical properties of long maize fiber reinforced polypropylene composites, *Trans. MRSJ* **26**, 1083–1090 (2001).
28. A. Kasuya, H. Hamada and A. Nakai, Molding and mechanical properties of unidirectional natural spun natural fiber-reinforced thermoplastics by spun yarn, in: *Proc. Annu. Conf. Japan Society for Composite Materials*, Tokyo, Japan, pp. 7–8 (2005) (in Japanese).
29. N. G. McCrum, C. P. Buckley and C. B. Bucknall, *Principles of Polymer Engineering*. Oxford University Press, Oxford (1988).
30. W. Weibull, A statistical distribution function of wide applicability, *J. Appl. Mech.* **18**, 293–297 (1951).
31. D. Hull, *An Introduction to Composite Materials*. Cambridge University Press, Cambridge (1981).
32. S. W. Tsai and H. T. Hahn, *Introduction to Composite Materials*. Technomic Publishing, Westport (1980).